Tunable liquid microlens arrays in electrode-less configuration and their accurate characterization by interference microscopy

L. Miccio, A. Finizio, S. Grilli, V. Vespini, M. Paturzo, S. De Nicola, and Pietro Ferraro
Istituto Nazionale di Ottica Applicata (CNR-INOA) & Istituto di Cibernetica del CNR "E. Caianiello",

Via Campi Flegrei 34 – 80078 Pozzuoli (NA), Italy
simonetta.grilli@inoa.it, lisa.miccio@inoa.it, pietro.ferraro@inoa.it

Abstract: A special class of tunable liquid microlenses is presented here. The microlenses are generated by an electrowetting effect under an electrode-less configuration and they exhibit two different regimes that are named here as separated lens regime (*SLR*) and wave-like lens regime (*WLR*). The lens effect is induced by the pyroelectricity of polar dielectric crystals, as was proved in principle in a previous work by the same authors (S. Grilli et al., Opt. Express 16, 8084, 2008). Compared to that work, the improvements to the experimental set-up and procedure allow to reveal the two lens regimes which exhibit different optical properties. A digital holography technique is used to reconstruct the transmitted wavefront during focusing and a focal length variation in the millimetre range is observed. The tunability of such microlenses could be of great interest to the field of micro-optics thanks to the possibility to achieve focus tuning without moving parts and thus favouring the miniaturization of the optical systems.

OCIS codes: (010.1080) Adaptive optics; (220.3630) Lenses; (160.3730) Lithium niobate (090.0090) Holography.

References and links

1. L. Dong, A. k. Agarwal, D. J. David, J. Beebe, and H. Jiang, "Adaptive liquid mcrolenses activated by stimuli-responsive hydrogels," Nature **442**, 551-554 (2006).
2. B. Berge and J. Peseux, "Variable focal lens controlled by an external voltage: An application of electrowetting," Eur. Phys. J. E **3**, 159-163 (2000).
3. L. G. Commander, S. E. Day, and D. R. Selviah, "Variable focal length microlenses," Opt. Comm. **17**, 157-170 (2000).
4. P. H. Huang, T. C. Huang, Y. T. Sun, and S. Y. Yang, "Fabrication of large area resin microlens arrays using gas-assisted ultraviolet embossing," Opt. Express **16**, 3041-3048 (2008).
5. A. Pikulin N. Bityurin, G. Langer, D. Brodoceanu, and D. Bauerle, "Hexagonal structures on metal-coated two-dimensional microlens arrays," Appl. Phys. Lett. **91,** 191106 (2007).
6. F. Krogmann, W. Monch, and H. Zappe, "A MEMS-based variable micro-lens system," J. Opt. A **8**, S330-S336 (2006)
7. C. C. Cheng, C. A. Chang, and J. A. Yeh, "Variable focus dielectric liquid droplet lens," Opt. Express **14**, 4101-4106 (2006)
8. C. C. Cheng and J. A. Yeh, "Dielectrically actuated liquid lens," Opt. Express **15**, 7140-7145 (2007).
9. N. Chronis, G. L. Liu, K. H. Jeong, and L. P. Lee, "Tunable liquid-filled microlens array integrated with microfluidic network," Opt. Express **11**, 2370-2378 (2003).
10. D. Y. Zhang, N. Justis, and Y. H. Lo, "Integrated fluidic adaptive zoom lens," Opt. Lett. **29**, 2855-2857 (2004).
11. P. M. Moran, S. Dharmatilleke, A. H. Khaw, K.W. Tan, M. L. Chan, and I. Rodriguez, "Fluidic lenses with variable focal length," Appl. Phys. Lett. **88**, 041120 (2006).
12. H. Ren, D. Fox, P. A. Anderson, B. Wu, and S.T. Wu, "Tunable-focus liquid lens controlled using a servo motor," Opt. Express **14**, 8031-8036 (2006).
13. L. Hou, N. Smith, and J. Heikenfeld, "Electrowetting Modulation of Any Flat Optical Film," Appl. Phys. Lett. **90**, 251114 (2007).

#103222 - $15.00 USD Received 24 Oct 2008; revised 12 Dec 2008; accepted 19 Dec 2008; published 6 Feb 2009

14. N. Smith, D. Abeysinghe, J. Heikenfeld, and J. W.Haus, Agile, "Wide-Angle Beam Steering with Electrowetting Microprisms," Opt. Express **14**, 6557 (2006).
15. B. Sun, K. Zhou, Y. Lao, W. Cheng, and J. Heikenfeld, "Scalable Fabrication of Electrowetting Pixel Arrays with Self-Assembled Oil Dosing," Appl. Phys. Lett. **91**, 011106 (2007).
16. S. Kuiper and B. H. W. Hendriks, "Variable- focus liquid lens for miniature cameras," Appl. Phys. Lett. **85**, 1128-1130 (2004).
17. J. L. Lin, G. B. Lee, Y. H. Chang, and K. Y. Lien, "Model Description of Contact Angles in Electrowetting on Dielectric Layers," Langmuir **22**, 484-489 (2006).
18. W. H. Hsieh and J. H. Chen, "Lens-Profile Control by Electrowetting Fabrication Technique," IEEE Photon. Technol. Lett. **17**, 606-608 (2005).
19. G. Milne, G. D. M. Jeffries, and D. T. Chiu, "Tunable generation of Bessel beams with a fluidic axicon," Appl. Phys. Lett. **92**, 261101 (2008).
20. X. Mao, J. R. Waldeisen, B. K. Juluri, and T. J. Huang, "Hydrodynamically tunable optofluidic cylindrical microlens," Lab. Chip **7**, 1303-1308 (2007).
21. X. Huang, C. M. Cheng, L. Wang, B. Wang, C. C. Su, M. S. Ho, P. R. LeDuc, and Q. Lin, "Thermally tunable polymer microlenses," Appl. Phys. Lett. **92,** 251904 (2008).
22. Y. Lu and S. Chen, "Direct write of microlens array using digital projection photopolymerization," Appl. Phys. Lett. **92**, 041109 (2008).
23. W. Moench and H. Zappe, "Fabrication and testing of micro-lens arrays by all-liquid techniques," J. Opt. A **6**, 330-337 (2004).
24. Y. Choi, H. R. Kim, K. H. Lee, Y. M. Lee, and J. H. Kim, "A liquid crystalline polymer microlens array with tunable focal intensity by the polarization control of a liquid crystal layer," Appl. Phys. Lett. **91**, 221113 (2007).
25. H. Ren, Y. H. Fan, and S. T. Wu, "Liquid-crystal microlens arrays using patterned polymer networks," Opt. Lett. **29**, 1608-1610 (2004).
26. H. Ren and S. T. Wu, "Tunable-focus liquid microlens array using dielectrophoretic effect," Opt. Express **16**, 2646-2652 (2008).
27. K. H. Jeong, G. L. Liu, N. Chronis, and L. P. Lee, "Tunable microdoublet lens array," Opt. Express **12**, 2494-2500 (2004).
28. S. Grilli, L. Miccio, V. Vespini, A. Finizio, S. De Nicola, and P. Ferraro, "Liquid micro-lens array activated by selective electrowetting on lithium niobate substrates," Opt. Express **16**, 8084-8093 (2008).
29. M. Yamada, N. Nada, M. Saitoh, and K. Watanabe, "First-order quasi-phase matched $LiNbO_3$ waveguide periodically poled by applying an external field for efficient blue second-harmonic generation," Appl. Phys. Lett. **62**, 435-436 (1993).
30. S. Grilli, M. Paturzo, L Miccio, and P. Ferraro, "*In situ* investigation of periodic poling in congruent LiNbO3 by quantitative interference microscopy," Meas. Sci. Technol. **19**, 074008 (2008).
31. E. M. Bourim C. W. Moon, S. W. Lee, V. Sidorkin, and I. K. Yoo, "Pyroelectric electron emission from –Z face polar surface of lithium niobate monodomain single crystal," J. Electroceram **17**, 479-485 (2006).
32. P. Ferraro, S. De Nicola, and G. Coppola, "Digital holography: recent advancements and prospective improvements for applications in microscopy," in *Optical Imaging Sensors and Systems for Homeland Security Applications*, vol. 2 of *Advanced Sciences and Technologies for Security Applications* series B. Javidi ed., (Springer, 2005), pp. 47-84.

1. Introduction

Liquid lenses are becoming important optical devices for a wide variety of applications ranging from mobile-phone cameras to biology. Among others, their foremost advantage is the possibility to have variable focusing by adapting their shape [1-8]. In fact, the liquid shape can be effectively changed to obtain different radius of curvature and consequently a varying optical power. Essentially, up to now, only two procedures have been invented to change the shape of the liquid mass. The first one makes use of a container with a flexible and elastic membrane that changes its shape under hydrostatic and/or pneumatic forces [9-12]. This former physical principle is very simple to be understood and figured out. A completely different principle is instead adopted when using the electrowetting (EW) effect [13-18]. In the latter case electric forces are used to change the shape of the liquid volume thus adapting the lens focus. Basically, the electric charges at the liquid-liquid or at the solid-liquid interface, depending on the type of microsystem, induce a modification of the interfacial tension, leading to a new shape of the liquid mass.

Since long time the liquids have been considered good materials for realizing optical elements, such as liquid mirrors for large telescopes made with Hg contained into large pan, where the right parabolic shape was induced by appropriate rotary motion. However, only

#103222 - $15.00 USD Received 24 Oct 2008; revised 12 Dec 2008; accepted 19 Dec 2008; published 6 Feb 2009

recently the liquid lenses are being used for practical applications, thanks to the latest developments in micro-technology and material science. In fact, important advancements have been achieved in the development of liquid single lenses with a variable focal length. Such components will find wide practical applications even in consumer electronics, such as for the cameras of the cellular phones [16]. Recently, special liquid-based optics, such as axicon lenses, have been developed by using polymeric materials as liquid containers [19]. Cylindrical lenses with hydrodynamic tunability [20] and polymer lenses tuned thermally [21] have been also investigated and tested.

The EW manipulation of liquids has been also reported for angle tilting of suspended micro mirrors or gratings [14], for the realization of beam-steering devices [15] and displays [16]. However, even though many configurations have been demonstrated for single liquid lenses, very few cases are reported for liquid microlens arrays with variable focus. Microlens arrays can find important applications in medical stereo-endoscopy, imaging, telecommunication and optical data storage. The microlens arrays can be fabricated by using different approaches and materials. For example, direct photo-polymerization by digital projectors has been adopted in Ref. [22] or by using wettability on monomer layers in [23] but to fabricate microlens arrays with a fixed focal length.

A completely different category of microlens arrays is instead based on the liquid-crystals [24,25], where the birefringence is used to tune the lens through the change of the refractive index. However, here we limit the discussion to tunable liquid microlens arrays without liquid crystals.

Recently, two significant results have been reported on the design and fabrication of tunable liquid microlens arrays. The first one was developed by using the dielectrophoretic effect on two liquid layers made of water and oil [26]. The focal power of such microlenses was varied by the EW process and the focal lengths were reported in the range from about 1.5mm to 2.2mm. The microlenses had a diameter around 100-140 μm. The aberrations of such microlenses were calculated numerically by an optical code program, on the basis of the well known fabrication specifications and material parameters. The second noteworthy result, reported in Ref. [27], consists of an hybrid optical configuration made of solid microlenses combined with liquid filled lenses, thus obtaining a tunable doublet with minimal optical aberrations. The optical characterization was performed as a function of the applied pressure to the microfluidic apparatus. In fact, under fluid pressure, the elastomer (PDMS) membrane containing the liquid, experienced a deformation. An interferometric profilometer was used for measuring the height of the solid lenses whereas an optical microscope with monochromatic light was adopted to evaluate the *f*-number as a function of the hydrostatic pressure [27]. It is important to note that all of the aforesaid optical systems require the minimization of the aberrations which is achieved by a proper design and a subsequent accurate optical characterization. For example, the fabrication of the liquid microlens array by the two approaches mentioned above requires a relatively complicated process making use of different materials.

A recent work from the same authors presented a completely new approach demonstrating the proof of principle to obtain liquid microlenses using an EW process implemented under an electrode-less configuration [28]. The expression electrode-less configuration was used by the authors to underline that the substrate was functionalized so that the substrate itself behaves as electrodes. In this way the use of different materials is avoid. In fact, the electrodes were built into the crystal, used as substrate, through a micro-engineering process and were activated pyroelectrically by an appropriate temperature variation. The crystal employed was a periodically poled polar dielectric crystal (Lithium Niobate LN) [29, 30] was used as substrate and the formation of sessile microdroplets was driven by the patterned surface charges induced by the pyroelectric effect [31]. The fundamental physics responsible of the phenomenon leading to the formation of microdroplets was illustrated and investigated in Ref. [28]. In addition, that work presented very preliminary results on the investigation of the possible applications of those microdroplets for the fabrication of liquid microlenses. A preliminary optical characterization was carried out in order to estimate the focal length of the

#103222 - $15.00 USD Received 24 Oct 2008; revised 12 Dec 2008; accepted 19 Dec 2008; published 6 Feb 2009

microlenses during their relaxation state and an example of imaging application was also shown. However, even though the proof of principle of the liquid microlens array was demonstrated, the set-up implemented in that work did not provide a reliable control of the substrate temperature, thus preventing a true characterization of the liquid microlenses.

In this paper we describe the new results coming out from the investigations performed in addition to the work presented in Ref. [28]. In fact, the use of a more sophisticated experimental system revealed the possibility of obtaining two different lens regimes that are called here *separated lenses regime* (*SLR*) and *wave-like lenses regime* (*WLR*). In the first case the liquid microlenses are separated from each other due to the breakup of the liquid layer, while in the second case the oil film appears uniformly distributed over the sample with a curved profile in correspondence of specific regions. In addition, the possibility of focus tuning with different optical behaviours was investigated for each kind of microlenses.

Moreover, this paper reports on an accurate optical testing of the liquid microlenses with the aim at assessing their optical behaviour for exploiting them for practical applications. The system for temperature control and observation of the microlens arrays was considerably improved respect to the previous work [28], thus allowing to perform the above mentioned characterization by an accurate procedure for each kind of microlenses. The experimental data could be used to develop and verify more sophisticated theoretical models for the description of the wettability/dewettability process on the substrate. An interferometric technique has been used before for the optical testing of the microlenses but exclusively for measuring the profile of the solid microlenses rather than for checking directly the wavefront characteristics [23, 24]. Besides, the usual testing procedure reported for tunable liquid microlenses consists of relatively simple imaging experiments or focal spot analysis [21,22,26]. Here, to the best of our knowledge, it is the first time that an interferometric technique is used for testing directly a tunable liquid microlens array. The optical testing of the microlenses was performed by using an interferometric system based on digital holography (DH), under a microscope configuration. The advantage of using DH consists in testing the optical wavefront directly at the exit pupil of the lens by using holographic reconstruction. The optical third order aberrations at various temperatures were also evaluated experimentally.

2. Description of the two liquid microlens regimes: separated lenses regime (*SLR*) and wave-like lenses regime (*WLR*)

The possibility of producing liquid microlens arrays onto dielectric crystals has already been demonstrated by the authors in Ref. [28], where a detailed description of the technique and of the interpretation of the lens effect were presented and discussed. This paper is aimed at presenting two new regimes revealed in liquid lens formation on the basis of the preliminary lens effect discovered and illustrated in Ref. [28]. Furthermore, a complete characterization of the microlens arrays was obtained for the two regimes in terms of focusing behaviour and optical aberrations. A brief description of the samples and of the two microlens regimes is provided in this section. Both sides polished and 500 μm thick LN crystals were periodically poled by standard electric field poling [31,32] in order to achieve a square array of hexagonal reversed domains. A standard mask lithography process was used to generate the desired resist pattern and the subsequent application of high voltage pulses led to the formation of the reversed domain grating [28]. Figure 1(a) shows the optical microscope image of a typical PPLN sample used for the formation of the liquid microlenses. An appropriate temperature variation of the PPLN substrate generates the pyroelectric effect which causes the formation of uncompensated surface charges able to activate an EW effect. This phenomenon allows the formation of regular liquid lenses in correspondence of the hexagonal domains, as extensively described in Ref. [28]. Basically, the heating process makes the spontaneous polarization of the LN crystal to decrease, thus leaving uncompensated charges onto the crystal surface (positive charges in correspondence of the *z*- face and *viceversa*). Conversely, the cooling process makes the polarization to increase thus generating uncompensated polarization charges with opposite signs respect to the heating process (positive charges in correspondence

#103222 - $15.00 USD Received 24 Oct 2008; revised 12 Dec 2008; accepted 19 Dec 2008; published 6 Feb 2009

of the *z*+ face and *viceversa*). Such surface charge distributions generate an electric field responsible of the EW effect.

As mentioned into the previous section, two different regimes of the microlens array, *WLR* and *SLR*, were observed by the new control set-up used this work. Figure 1(b),(c) show the schematic views of the sample cross section under the *WLR* and the *SLR*, respectively. The black arrows indicate the orientation of the spontaneous polarization into the original (light grey) and reversed (dark grey) ferroelectric domains. The case reported in this figure refers to the cooling process, so that uncompensated negative charge is developed in correspondence of the negative side of the spontaneous polarization, and *viceversa*.

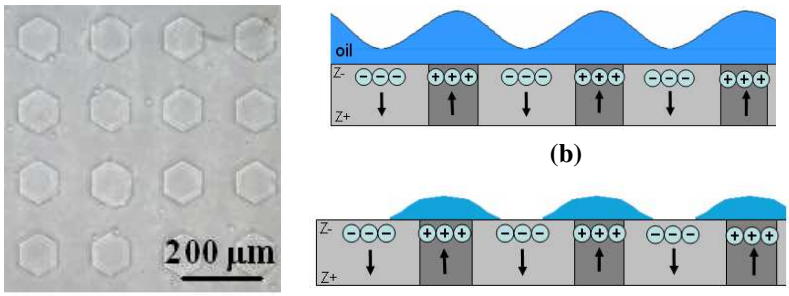

(a) (c)

Fig. 1. (a) Optical microscope image of a typical PPLN with a square array of hexagonal reversed domains; (b), (c) schematic views of the sample cross section corresponding to the *wave-like lenses regime* and to the *separated lenses regime* of the microlens array, respectively. In both cases the temperature of the substrate is decreasing. The difference between the two regimes stands in the liquid thickness. The black arrows indicate the orientation of the spontaneous polarization.

The *WLR* consists of an oil layer with a sinusoidal-like profile according to the electric field generated onto the crystal surface by the pyroelectric effect. Such profile results from the equilibrium condition achieved by the surface tensions at the solid-liquid and liquid-air interfaces in presence of the above mentioned electric potential, according to the numerical simulations performed in the previous work (see section 3 in Ref. [28]). Typically the liquid layer for obtaining the *WLR* ranges between 100 µm and 300 µm. Differently, the *SLR* is obtained by using a thinner layer of liquid onto the crystal surface, obtained by spinning the liquid onto the substrate. Having a thinner oil film the work performed by the charges is able, in this case, to break-up the film oil into the regions surrounding the hexagonal regions, thus forming isolated liquid microlenses. The layer thickness in the latter case was estimated to range from 10 µm to 25 µm. In the case of *WLR* the lens effect is due to a temporary waviness obtained at the liquid-air interface. The higher the amplitude of the waviness is, the stronger is the lens effect. The focal length in this case of each liquid lens goes from infinity to the minimum value obtained by the shorter curvature at the air-liquid interface. However the *WLR* is clearly a temporary configuration that disappears when the temperature returns back to its initial value. Tunable effect exploit this temporary effect, and the obtainable focal range depends from the temperature change as well as the liquid properties. On contrary the *SLR* exhibits a more stable behaviour. Nevertheless, due to the break-up of the liquid layer, the shape of the microlenses is different and the tunability varies correspondingly.

3. Experimental procedure

Both regimes were investigated by an interferometric technique based on a DH microscope set-up, in order to characterize the focusing behaviour and the optical aberrations of the microlenses. Figure 2 shows the schematic view of the interferometric apparatus used for the measurements.

#103222 - $15.00 USD Received 24 Oct 2008; revised 12 Dec 2008; accepted 19 Dec 2008; published 6 Feb 2009

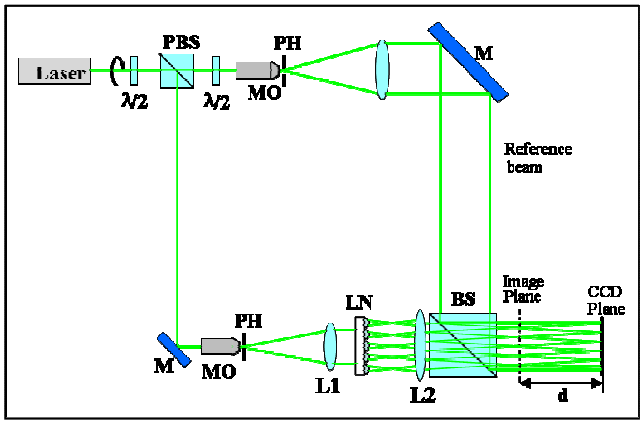

Fig. 2. Schematic view of the interferometric configuration. *PBS* polarizing beam splitter; *MO* microscope objective; *PH* pin-hole; *M* mirror; *BS* beam splitter.

The setup is based on a Mach-Zehnder type interferometer with a continuous laser source emitting at a wavelength of 532 nm. The sample is positioned on a thermo-controlled plate and put into the object arm of the interferometer. Before impinging on the sample the object beam is spatially filtered and expanded by means of the telescope system made of a microscope objective (MO), a pinhole (PH) and an achromatic doublet (L1). The light coming from the array is collected by a microscope objective, depicted in Fig.2 by lens L2, and made to interfere with the reference beam. The resulting interference patterns (holograms) are captured by the CCD camera that is placed far off the image plane of L2. The distance, *d*, between the CCD plane and the image plane is named reconstruction distance. An appropriate numerical manipulation of such interferograms allows one to retrieve information in the image plane about the complex wavefront, and thus about the phase and the intensity of the optical wavefield transmitted by the sample. Two sets of holograms were acquired during the temperature variation, corresponding to the heating and the cooling process. Such holograms were then elaborated numerically in order to reconstruct the phase distribution of the transmitted wavefront. Standard numerical procedures in DH image recontruction can be found in Refs. [30,32]. The reconstructed phase images corresponding to different instants of the heating or the cooling process were collected into movies showing the evolution of the wavefront curvature. These results allow one to retrieve information about the focal length variation *versus* the substrate temperature. The aberration characteristics of the liquid microlenses were obtained by a numerical fitting of the phase maps with appropriate polynomials describing different aberration terms.

All of the results reported in this paper have been obtained by using carboxylic acid (pentanoic acid - $C_5H_{10}O_2$) as the oily substance spread onto the *z*-cut $LiNbO_3$ substrates. The temperature of the thermo-controlled plate under the sample was varied with a rate of 10°C/min, that is lower than that estimated in the previous work (i.e. 20°C). Moreover, in this work the temperature was controlled with an accuracy of 0.1 °C and the interferometric characterization was performed by registering the temperature value for each digital hologram captured during the thermal treatment.

4. Results and discussion

This section presents the results achieved for the optical characterization of the tunable microlens array under both the *WLR* and the *SLR*. Two different kinds of analysis were carried out in order to evaluate the temperature dependence of the focal length and the optical aberrations of the lenses, thus characterizing both the tunability and the optical performance of the device. The temperature dependence of the focal length was investigated during the cooling and the heating treatments, which were considered as independent processes. It means

#103222 - $15.00 USD Received 24 Oct 2008; revised 12 Dec 2008; accepted 19 Dec 2008; published 6 Feb 2009

that the array is heated or cooled by means of temperature ramps. The aberrations of the lenses were evaluated through a complete analysis of the wavefronts transmitted by the lenses themselves.

4.1 Characterization of the tunable microlens array under WLR

This section reports the characterization results obtained in case of microlens arrays exhibiting a *WLR***.** Figure 3(a),(b) contain two movies showing the temporal evolution of the mod 2π spatial phase distribution corresponding to the heating (Media 1) and the cooling (Media 2) process, respectively. The temperature values range from 30°C to 90°C in both cases. The thermo controlled plate is made of a calibrated Peltier cell whose temperature is driven by software. Moreover the system is provided with an NTC thermistor as temperature sensor. The temperature we measure is the temperature of the whole lens array.

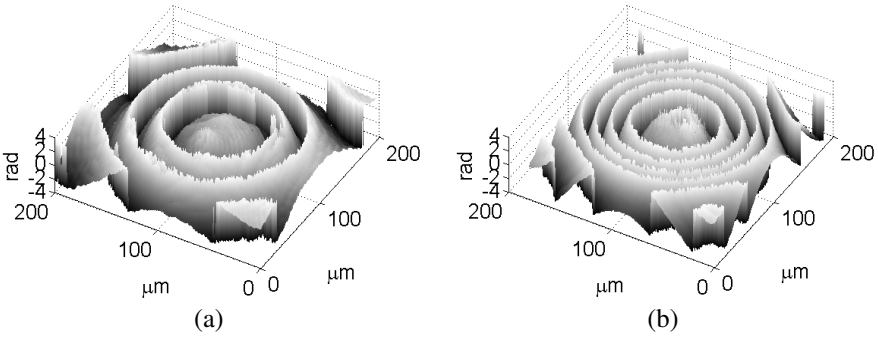

Fig. 3. Movies showing the evolution of the wrapped mod 2π phase map during (a) the heating (Media 1) and (b) the cooling process (Media 2).

The movies clearly show that the wrapped phase maps exhibit a different behaviour. In case of rising temperature (see Fig. 3(a) (Media 1)) the number of fringes increases only during the first part of the process, up to a temperature value of about 65°C, and then stabilizes. Conversely, during the cooling process (see Fig. 3(b) (Media2)), the number of fringes increases during the whole process. An unwrapping numerical procedure was applied to the phase *mod* 2π in order to retrieve the real phase distribution of the wavefront. Successively, a one-dimensional fitting procedure was carried out to calculate the focal length of the microlens according to the following equation:

$$\Phi(x) = \frac{\pi}{\lambda}\frac{\left(x^2\right)}{f} \tag{1}$$

Figure 4(a),(b) show the experimental and the corresponding fitted profiles of the unwrapped phase corresponding to the temperature increase and decrease, respectively. The clearly visible step-like profile exhibited by the lower curves correspond to the hexagon domain walls. This step is due to the electro-optic effect induced through the pyroelectric effect [30]. The variation of the focal length as a function of the temperature is reported in Fig. 4(c),(d), for the heating and the cooling process, respectively. The results show that the lens effect is more pronounced during the cooling process with a focal length value ranging from 16 mm down to 1.5 mm, corresponding to a temperature variation between 90°C and 35°C. The behaviour during heating exhibits a focal length variation from 8.7 mm down to 2 mm while the temperature rises from 35°C up to 65°C and then stabilizes in agreement with the previous observation on the wrapped phase maps.

#103222 - $15.00 USD Received 24 Oct 2008; revised 12 Dec 2008; accepted 19 Dec 2008; published 6 Feb 2009

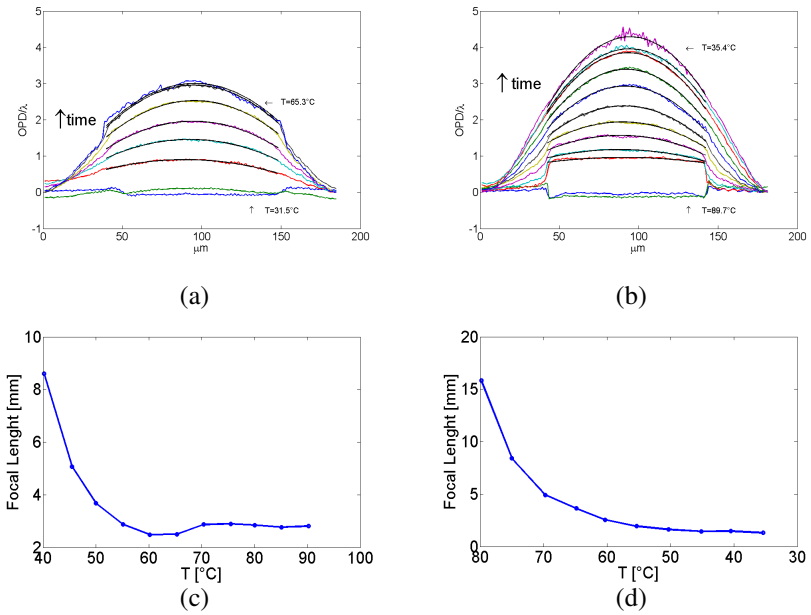

Fig. 4. Experimental and fitted 1D profiles of the unwrapped phase distribution corresponding to (a) the heating and (b) cooling process; (c) (d) focal length variation as a function of temperature in case of the heating and the cooling process, respectively.

The optical behaviour of the microlenses was characterized also in terms of the optical aberrations intrinsically present in the lens array, by applying a two-dimensional fitting procedure. Several holograms of a 4×4 lens array were acquired during the stationary condition, i.e. when the number of fringes is stable in the wrapped phase distribution, while the fitting procedure was performed for each of the three chosen lenses of the array and for the lenses of some arrays at different time instants.

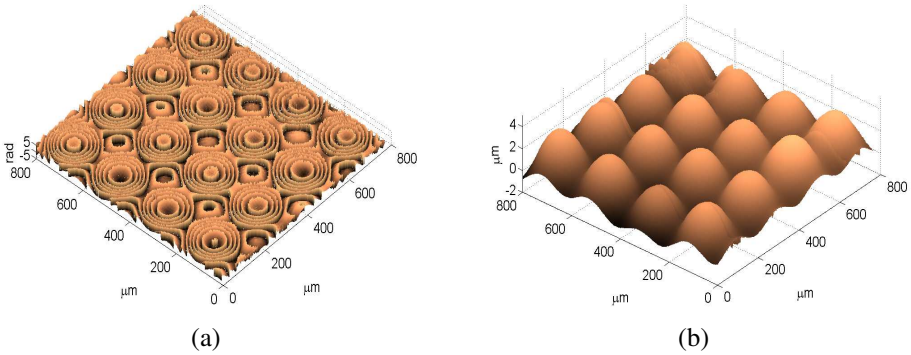

Fig. 5. Two-dimensional representation of (a) the wrapped and (b) the unwrapped phase map corresponding to 4×4 microlens array.

Figure 5(a),(b) show the wrapped and the unwrapped phase map of the whole wavefront transmitted by the lens array, respectively. The function used for the fitting process is a linear combination of Zernike polynomials. The measured and the calculated phase distribution are presented in Fig. 6(a),(b), respectively. The coefficients of the linear combination for the tilts, the astigmatism, the focus, and the third order spherical aberration terms were evaluated. The coma and the higher order coefficients were neglected because smaller of some orders of

#103222 - $15.00 USD Received 24 Oct 2008; revised 12 Dec 2008; accepted 19 Dec 2008; published 6 Feb 2009

magnitude. The coefficients for some different lenses are reported in Tab. 1. The calculated coefficients show that the phase distribution at the exit of each lens is made of the same terms for each lens and, for each term of the linear expansion, the coefficients of different lenses are similar. This allows us to state that our device displays the same properties for each microlens.

Table 1. List of coefficient values.

	Array 1			Array2
	Lens A	Lens B	Lens C	Lens B
Constant Term A	3.21	3.23	3.96	2.75
Tilt about x (10^{-4}) x	25.0	8.54	21.0	-22.0
Tilt about y (10^{-4}) y	-82.0	-94	-45.0	-31.0
Astigmatism with axis at 45° (10^{-6}) 2xy	-2.90	-3.88	0.84	-5.61
Defocus (10^{-4}) $-1+2y^2+2x^2$	-9.26	-7.23	-7.46	-6.91
Astigmatism with axis at 0° or 90° (10^{-5}) y^2-x^2	-5.57	1.46	-3.78	2.56
Triangular Astigmatism on x axis (10^{-8}) $3xy^2-x^3$	-0.29	6.50	-1.94	31.97
Triangular Astigmatism on y axis (10^{-7}) y^3-3x^2y	-4.27	-5.38	-0.62	-1.61
Third Order spherical aberration (10^{-8}) $1-6y^2-6x^2+6y^4+12x^2y^2+6x^4$	3.61	2.77	2.57	3.02

Figure 6 shows the surface distribution of each polynomial that contributes to the fitted surface for a single lens, in order to compare the focus term to the other terms which describe the wavefront curvature. In particular, Fig. 6(c) displays the focus term, which is the main term contributing to the phase distribution. Figure 6(d) shows the distribution of the third order spherical aberration that appears flat in the central region while diverging in the peripheral one. This divergence is due to the oil layer existing between adjacent lenses, in fact the oil layer redistributes its mass during the temperature variation but, in this case, without breaking up between adjacent lenses. Figure 6(e),(f),(g),(h) show the distributions of the astigmatism terms.

The information provided by Figure 6(d) and Table 1 reveal that the spherical aberration term has a quite high value with the main contribution due to the intrinsic waviness at the air-liquid interface in between two adjacent microlenses where the curvature changes from convex to concave.

#103222 - $15.00 USD Received 24 Oct 2008; revised 12 Dec 2008; accepted 19 Dec 2008; published 6 Feb 2009

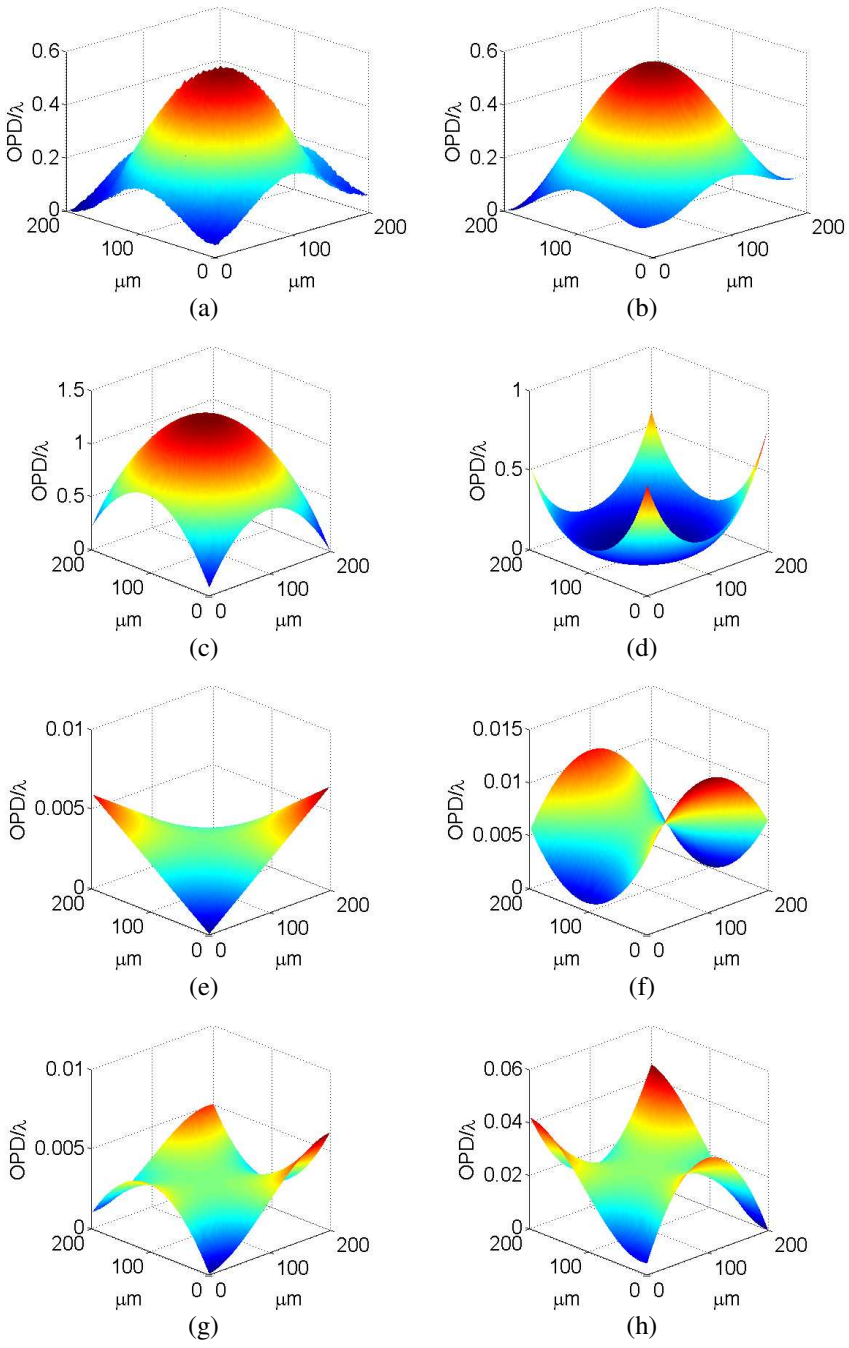

Fig. 6. (a) Measured phase distribution and (b) corresponding fitted surface; surface distribution of (c) the focus term, (d) the third order spherical aberration, (e) the astigmatism at 45° term, (f) the astigmatism at 90°, (g) the triangular astigmatism on *x* base, (h) the triangular astigmatism on *y* base.

#103222 - $15.00 USD Received 24 Oct 2008; revised 12 Dec 2008; accepted 19 Dec 2008; published 6 Feb 2009

4.2 Characterization of the tunable microlens array under SLR

A similar analysis was carried out in case of the *SLR*. Figures 7(a) and 7(b) show the movies of the two-dimensional wrapped phase distribution corresponding to this configuration for a portion of 4×4 microlenses evolving during the heating (Media 3) and the cooling (Media 4) treatments, respectively. In Fig.7(a)(Media 3) the temperature varies form 25.6 °C to 79.0 °C. As can be noticed in the movie, while the temperature reaches 57°C (at about half of the duration of the movie) the liquid layer breaks up and the flat surface of the substrate becomes visible. At the end of the movie, corresponding to about 79.0°C, the liquid droplets are clearly separated. Conversely, the movie in Fig.7(b) (Media 4) shows the behaviour of the open microfluidic system while the temperature changes between 79.3°C and 34.4°C. When the temperature reaches 34.4°C the lens effect disappears completely and the liquid layer relaxes.

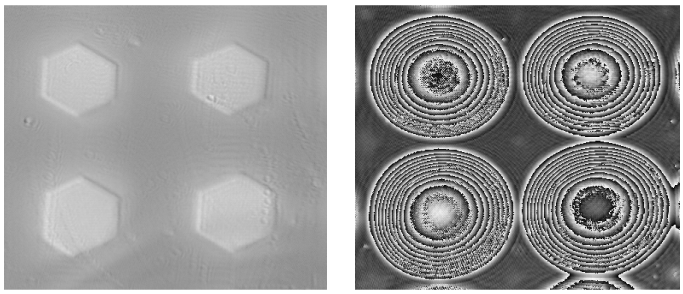

(a) (b)

Fig. 7. Movies of the wrapped phase distribution evaluated for a portion of the lens array in case of separated lenses SRL (a) heating (Media 3) and (b) cooling (Media 4).

The number of fringes is clearly higher compared to the case of the *WLR* and their density increases from the central to the side region of the lenses. This means that, in case of *SL*, the slope is more pronounced in correspondence of the peripheral regions and that the lenses are relatively flat in the centre.

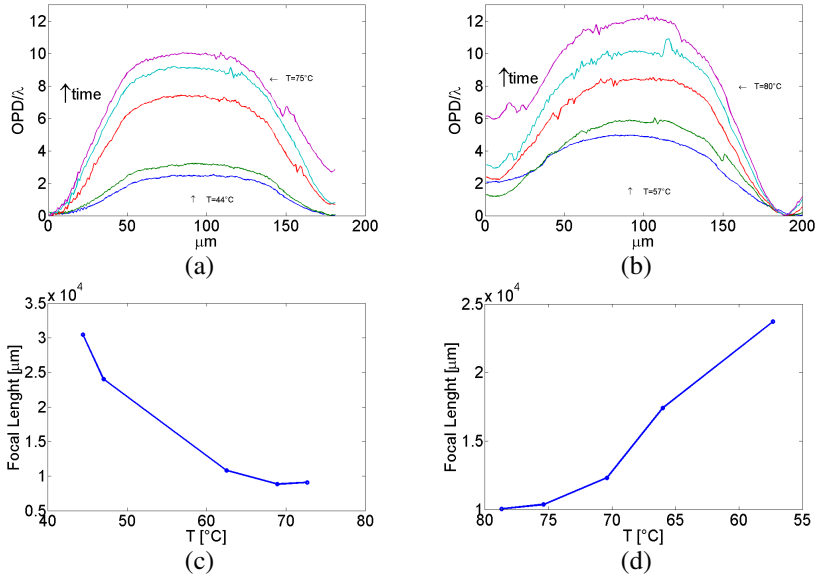

Fig. 8. Profile of the phase distribution during (a) heating and (b) cooling; (c),(d) temperature dependence of the focal length for the heating and the cooling process, respectively, in case of separated lenses.

#103222 - $15.00 USD Received 24 Oct 2008; revised 12 Dec 2008; accepted 19 Dec 2008; published 6 Feb 2009

This behaviour is proved by the unwrapped phase profiles shown in Fig. 8(a),(b), where the two pictures refer to the heating and the cooling process, respectively.
As in the previous case, the cooling treatment leads to a more pronounced phase variation compared to that occurring during heating, while the focal length values range between around 30 mm and 10 mm in both processes (see Fig. 8(c),(d)). The values of the focal length at the end of both processes is one order of magnitude higher than in case of *WLR*, due to the flatness of the oil profile in the centre of the lenses.

The aberrations were evaluated by a one-dimensional fitting of the wavefronts and Fig. 9(a) shows the measured and the fitted phase profile. Differently from the analysis carried out for the *WLR*, the high frequency of the fringes makes the two-dimensional unwrapping procedure very difficult to be accomplished, so that the following equation was used for the fitting procedure:

$$\boldsymbol{W}(\boldsymbol{x}) = \boldsymbol{a}(1)\boldsymbol{x}^4 + \boldsymbol{a}(2)\boldsymbol{x}^2 + \boldsymbol{a}(3)\boldsymbol{x} + \boldsymbol{a}(4) \tag{2}$$

where $\boldsymbol{W}(\boldsymbol{x})$ is the OPD. The calculated coefficients are reported in Fig. 9(b).

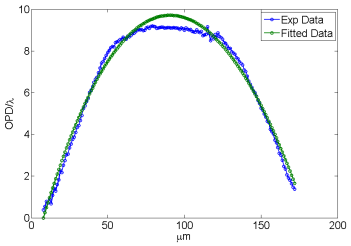

(a)

Coefficient	Value	Meaning
a(1)	-2.8×10^{-9}	Spherical Aberration Coefficient
a(2)	-6.2×10^{-4}	Defocusing Coefficient
a(3)	-0.0763	Tilt Coefficient
a(4)	2.7918	Constant Term

(b)

Fig. 9. (a) Measured and fitted phase profile; (b) list of the coefficient values of the linear expansion resulting from the fitting process.

The typical appearance of a single microlens under the *SLR* is shown by the optical microscope movie in Fig. 10 (Media 5), where the oil breakup between adjacent lenses is clearly visible.

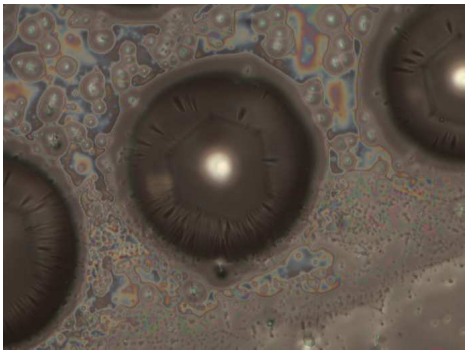

Fig. 10. Optical microscope movie (Media 5) of a single liquid lens of an array of separated lenses after formation and successive thermal tuning.

In this case the sample was observed under the microscope after treating thermally the microlens array already formed by the previous heating of the oil coated PPLN substrate. The movie shows the slight morphology variation experienced by the microlens during this

#103222 - $15.00 USD Received 24 Oct 2008; revised 12 Dec 2008; accepted 19 Dec 2008; published 6 Feb 2009

experiment, thus demonstrating the possibility to achieve a focus tuning of the microlenses after their formation. This effect may be of great interest to the field of optics, as demonstrated by some works presented recently in literature on this subject [21]. In fact, microlenses with adjustable focal lengths may be useful to eliminate the need for mechanically moving parts, thus reducing the size of the optical systems while enabling precision focusing. Anyway, further experiments, aimed at controlling better such fine-tuning, are currently under investigation. Moreover, it is important to note that the movie in Fig. 10 shows how, in case of the *SLR*, the evolution of the focal length is only slightly visible by the simple observation under the optical microscope. Conversely, the phase reconstruction in Fig. 7 clearly shows the curvature variation during the thermal process, thus demonstrating the importance of the DH technique for a deep understanding of the optical behaviour of such liquid microlenses.

5. Conclusions

The results presented in this paper show the possibility of obtaining tunable liquid microlens arrays by an EW effect obtained under an electrode-less configuration. The liquid microlenses are fabricated by manipulating the surface tension of appropriate oil films through the surface charges generated by the pyroelectric effect in PPLN substrates. The novel results show that two different microlens regimes can be obtained whenever the temperature is controlled accurately. The phenomena have been investigated and discussed. Basically the oil film thickness determines the generation of separated or wave-like lenses which exhibit different optical properties. Moreover, differently from the previous work reported in ref. [28] it emerges that clear focusing effect can be obtained even during the heating step. This is attributed to the lower heating rate of 10°C/min in respect to the previous one of 20°C/min. The accurate interferometric characterization was motivated by the necessity to have information about the properties of the dynamic focusing behaviour but also with the aim at understanding deeper the physics of the phenomenon. The results show that the focal length variation ranges between 16 mm and 1.5 mm and between 30 mm and 10 mm in case of the *WLR* and the *SLR*, respectively. An accurate optical investigation of the microlenses has been performed by a DH based technique, in order to characterize the properties of the liquid microlenses in terms of both focal length tunability and optical aberrations. The tunability of such microlenses could be of great interest to the field of micro-optics thanks to the possibility of achieving focus tuning without moving parts and thus favouring the miniaturization of the optical systems.

Acknowledgments

The research leading to these results has received funding from the European Community's Seventh Framework Programme FP7/2007-2013 under grant agreement n° 216105 “Real 3D”.

#103222 - $15.00 USD Received 24 Oct 2008; revised 12 Dec 2008; accepted 19 Dec 2008; published 6 Feb 2009